Bulgarian Chemical Communications, Volume 50, Special Issue F (pp. 115–125) 2018

Antibacterial activity of novel quaternary ammonium salts of quinoline and 4-pyrolidino pyridine

R. I. Rusew[1], V. B. Kurteva[2], B. L. Shivachev[1]

[1] *Institute of Mineralogy and Crystallography "Acad. Ivan Kostov", Bulgarian Academy of Sciences, Acad. G. Bonchev str., bl. 107, 1113 Sofia, Bulgaria*
[2] *Institute of Organic Chemistry with Centre of Phytochemistry, Bulgarian Academy of Sciences, Acad. G. Bonchev str., bl. 9, 1113 Sofia, Bulgaria*

Received October 23, 2018; Accepted November 30, 2018

Three new quaternary ammonium compounds were synthesized by Menshutkin reaction adapted for aromatic tertiary amines. The purity of the novel compounds was confirmed by ^{1}H-NMR and ^{13}C NMR spectroscopic techniques. Single crystal X-ray diffraction studies showed that all three compounds crystalize in the monoclinic crystal system (two in $P2_1/c$ and one in $P2_1/n$ space group) as bromide or iodide salts. The crystal structures are stabilized by a network of strong intermolecular halogen bonding interaction of C-H…X type (X = I, Br). DTA/TGA analyzes confirmed the stabilizing role of the counter ion by showing that the compounds decompose immediately after the elimination of the halogen atom. The quaternary ammonium compounds were tested for antibacterial activity against Gram-positive and Gram-negative bacterial strains using Kirby-Bauer disk diffusion test. Antibacterial effect was observed only on Gram-positive bacteria namely *Bacillus subtilis* and *Staphylococcus aureus*. The minimum inhibitory (MIC) and non-inhibitory (NIC) concentrations for all three compounds were obtained using the Gompertz function. Compound **2** showed the best results with MIC values of 0.321, 0.504 μM and NIC values of 0.053, 0.030 μM for *S. aureus* and *B. subtilis* respectively.

Keywords: Quaternary ammonium salts, Menshutkin reaction, Single-crystal X-ray diffraction, NMR, DTA\TGA, halogen bonding, antibacterial properties.

INTRODUCTION

Quaternary ammonium salts (QAS) have a "head" with a positively charged nitrogen atom that forms four chemical bonds with different alkyl, aryl and alkenyl substituents e.g. the "tail". QASs are usually synthesized by Menshutkin reaction [1] that refers to alkylation of tertiary amines with an alkyl halide [2]. The reaction yield is enhanced by polar aprotic solvents such as 1,2-dichlororethane or acetonitrile that helps the formation of solvated product [3]. Other methods for QAS synthesis include quaternization with dimethyl sulfate [4, 5] which is toxic and carcinogenic [6] or with dimethyl carbonate [7, 8] which is ecofriendly but gives lower yields. QASs have found various applications as cationic surfactants [9], phase-transfer catalysts [10], fabric softeners [11] etc. In addition, QAS constitute the cationic part of the majority ionic liquids [12, 13] as well as antibacterial agents. The increased drug resistance of bacteria as a consequence of excessive and improper use of antibiotics and the lack of "new" antibacterial drugs to overcome that resistance is a concerning tendency [14]. The most important mechanisms of bacterial resistance to antibiotics are gene mutations [15, 16] and horizontal gene transfer (HGT) [17, 18]. In order to evade those defensive mechanisms, researchers seek out different types of compounds, natural or synthetic, that have improved or unaffected antimicrobial properties [19–21]. It has been acknowledged that quaternary ammonium compounds that feature a "long aliphatic chain" (aliphatic groups with 8–18 carbons) possess antibacterial activity against Gram-positive, Gram-negative bacteria, as well as against some fungal strains and protozoa [22–25]. The antimicrobial action of QAS is based on their surfactant nature and begins when they reach the surface of the bacterial cell. When QAS are sufficiently close to the membrane they interact through hydrophobic and electrostatic attraction with the negatively charged bacterial cell surfaces. After their adsorp-

* To whom all correspondence should be sent:
Email: r.rusev93@gmail.com

tion on the outer of the cell, QAS molecules replace Ca^{2+} and Mg^{2+} ions from the cytoplasmic membrane [26]. This ion exchange destabilizes the intracellular matrix of the bacterium and leads to leakage of intracellular fluids [26]. The antimicrobial activity of QAS may also include destruction and denaturation of structural proteins and enzymes in the cell [27]. These processes inevitably lead to bacterial death. However, the lethal and inhibitory effects of quaternary ammonium compounds are strongly dependent on environmental factors – pH, temperature, ions concentration, etc. [28]. Their activity is enhanced at higher temperatures, continuous administration and presence of chelating agents but rapidly decreases in water/solutions rich in mineral salts [28]. The main concerns of QAS antibacterial activity are the ability of some multidrug resistant bacteria to block the penetration or export the drug through the cell membrane. This process is called "efflux" and it is carried out by "efflux-pump" proteins [29, 30].

The present work is focusing on a facile one step synthesis and structural characterization of new QAS and a study on their antimicrobial activity. The new QAS combines quinoline, 4-methyl quinoline and 4-pyrolidino pyridine moieties that will serve as a starting base for structure activity relationship (SAR) evaluation.

MATERIALS AND METHODS

Synthesis

All reagents were purchased from Alfa Aesar, Sigma Aldrich, Fluka and Riedel-de Haën and were used without further purification. The deuterated solvents were purchased from Deutero GmbH. The NMR spectra were recorded on a Bruker Avance II+ 600 spectrometer (Rheinstetten, Germany), ^{1}H at 600 MHz and ^{13}C at 151 MHz, in DMSO-d_6; the chemical shifts were quoted in ppm in δ-values against tetramethylsilane (TMS) as an internal standard and the coupling constants were calculated in Hz. The spectra were processed with Topspin 2.1 program.

Synthesis of 1-(2-(naphthalen-2-yl)-2-oxoethyl) quinolin-1-ium bromide – (1)

Quinoline (60 µl, 65 mg, 0.5 mmol) and 2-bromo-2'-acetonapthone (125 mg, 0.5 mmol) were dissolved in 1,2-dichloroethane (10 ml). The reaction was performed under inert atmosphere (argon) at ambient temperature. Orange precipitate was formed after 24h that was filtered and washed with 1,2-dichloroethane. Yield: 135 mg (65%) – Naphthalene ring is depicted as "prime". ^{1}H NMR 7.172 (s, 2H, CH_2), 7.732 (ddd, 1H, J 1.2, 7.0, 8.1, CH-7'), 7.780 (ddd, 1H, J 1.2, 7.0, 8.2, CH-6'), 8.078 (m, 2H, CH-6 + CH-3'), 8.102 (d, 1H, J 8.2, CH-5'), 8.170 (d, 1H, J 8.6, CH-4'), 8.229 (ddd, 1H, J 1.4, 6.9, 8.8, CH-7), 8.251 (d, 2H, J 8.2, CH-8'), 8.357 (dd, 1H, J 5.8, 8.4, CH-3), 8.517 (d, 1H, J 8.9, CH-8), 8.576 (dd, 1H, J 1.1, 8.2, CH-5), 8.986 (s, 1H, CH-1'), 9.477 (d, 1H, J 8.3, CH-4), 9.587 (dd, 1H, J 1.2, 5.8, CH-2); ^{13}C NMR 63.53 (CH_2), 119.45 (CH-8), 122.54 (CH-3), 123.74 (CH-3'), 127.79 (CH-7'), 128.23 (CH-5'), 129.01 (CH-4'), 129.61 (C_q-4a), 129.79 (CH-6'), 130.06 (CH-8'), 130.31 (CH-6), 130.97 (CH-5), 131.29 (C_q-2'), 131.57 (CH-1'), 132.37 (C_q-8a'), 135.88 (C_q-4a'), 136.32 (CH-7), 138.82 (C_q-8a), 148.98 (CH-4), 151.29 (CH-2), 190.88 (C=O).

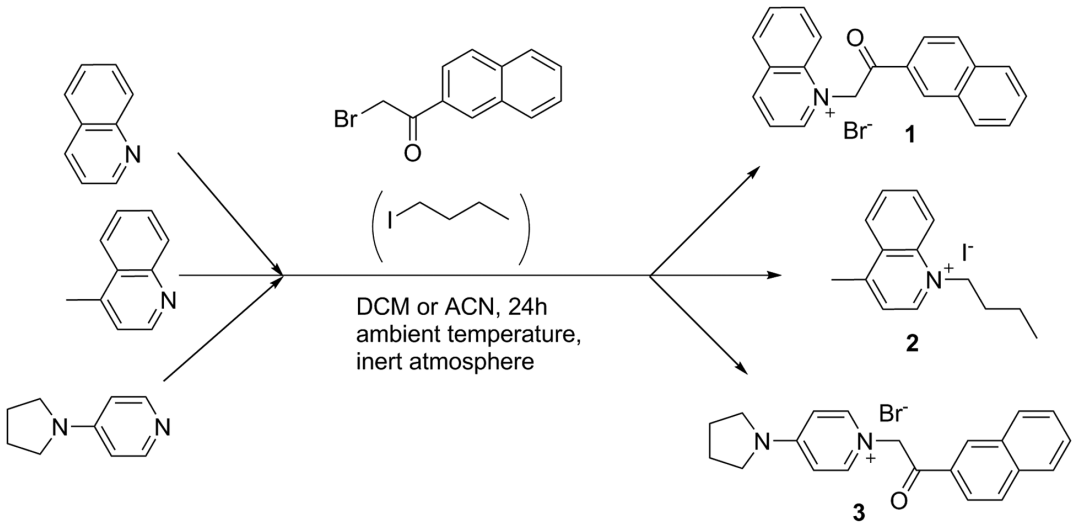

Scheme 1. General scheme of the synthetic procedure.

Synthesis of 1-butyl-4-methylquinolin-1-ium iodide – (2)

4-methyl quinoline (67 µl, 72 mg, 0.5 mmol) and 1-iodobutane (57 µl, 92 mg, 0.5 mmol) were mixed in acetonitrile (10 ml). The reaction was performed under inert atmosphere (argon) at ambient temperature. Green precipitate was formed after 24 h that was filtered and washed with acetonitrile. Yield: 128 mg (78%) – Butyl chain is depicted as "prime". ^{1}H NMR 0.905 (t, 3H, J 7.4, CH_3-4'), 1.387 (m, 2H, CH_2-3'), 1.917 (m, 2H, CH_2-2'), 3.003 (d, 3H, J 0.4, CH_3-4), 5.028 (t, 2H, J 7.5, CH_3-1'), 8.047 (ddd, 1H, J 8.4, 7.0, 0.8, CH-6), 8.090 (dd, 1H, J 6.0, 7.0, 0.7, CH-3), 8.255 (ddd, 1H, J 8.9, 6.9, 1.4, CH-7), 8.537 (dd, 1H, J 8.5, 1.2, CH-5), 8.616 (d, 1H, J 8.9, CH-8), 9.469 (d, 1H, J 6.0, CH-2); ^{13}C NMR 13.42 (CH_3-4'), 19.10 (CH_2-3'), 19.79 (CH_3-4), 31.38 (CH_2-2'), 56.72 (CH_2-1'), 119.38 (CH-8), 122.61 (CH-3), 127.15 (CH-5), 128.91 (C_q-4a), 129.56 (CH-6), 135.09 (CH-7), 136.64 (C_q-8a), 148.28 (CH-2), 158.48 (C_q-4).

Synthesis of 1-(2-(naphthalen-2-yl)-2-oxoethyl)-4-(pyrrolidin-1-yl) pyridin-1-ium bromide – (3)

4-pyrolidino pyridine (75 mg 0.5 mmol) and 2-bromo-2'-acetonapthone (125 mg, 0.5 mmol) were dissolved in acetonitrile (10 ml). The reaction was performed under inert atmosphere (argon) at ambient temperature. After 24h white precipitate was formed that was filtered and washed with acetonitrile. Yield: 158 mg (77%) – Pyrrolidine ring is depicted as "prime", naphthalene ring as "second". ^{1}H NMR 2.040 (m, 4H, CH_2-3'+4'), 3.551 (m, 4H, CH_2-2'+5'), 6.105 (s, 2H, CH_2), 7.003 (d, 2H, *J* 7.7, CH-3+5), 7.696 (ddd, 1H, *J* 1.2, 6.9, 8.1, CH-7"), 7.746 (ddd, 1H, *J* 1.2, 6.9, 8.1, CH-6"), 8.025 (dd, 1H, *J* 1.7, 8.6, CH-3"), 8.070 (d, 1H, *J* 8.0, CH-5"), 8.133 (d, 1H, *J* 8.7, CH-4"), 8.198 (d, 1H, *J* 8.1, CH-8"), 8.229 (d, 2H, *J* 7.7, CH-2+6), 8.790 (s, 1H, CH-1"); ^{13}C NMR 24.54 (CH_2-3'+4'), 48.16 (CH_2-2'+5'), 62.31 (CH_2), 107.76 (CH-3+5), 122.94 (CH-3"), 127.26 (CH-7"), 127.72 (CH-5"), 128.57 (CH-4"), 129.11 (CH-6"), 129.42 (CH-8"), 130.07 (CH-1"), 131.54 (C_q-2"), 132.34 (C_q-8a"), 135.61 (C_q-4a"), 142.99 (CH-2+6), 153.45 (C_q-4), 192.77 (C=O).

Single crystal X-ray diffraction

Suitable single crystals of the quaternary ammonium compounds were mounted on glass capillaries. The intensity and diffraction data were collected on Agilent SupernovaDual diffractometer equipped with an Atlas CCD detector using micro-focus Mo*K*α / Cu*K*α radiation (λ = 0.71073/1.54184 Å, respectively). The structures were solved by direct methods and refined by the full-matrix least-squares method on F^2 with ShelxS and ShelxL programs [31]. All non-hydrogen atoms, including solvent molecules, were located successfully from Fourier map and were refined anisotropically. Hydrogen atoms were placed at calculated positions using a riding scheme (*Ueq* = 1.2 for C-$H_{aromatic}$ = 0.93 Å and C-$H_{methylene}$ = 0.97 Å). The ORTEP [32] views of the molecules present in the asymmetric unit and the most important crystallographic parameters from the data collection and refinement are shown in Fig. 1 and Table 1 respectively. Selected bonds lengths, angles and torsion angles are given in Table 2. The figures concerning crystal structure description and comparison were prepared using Mercury software (version 3.9) [33].

Differential Thermal Analysis (DTA) and Thermogravimetric Analysis (TGA)

DTA and TGA were performed on Stanton Redcroft 1500 STA (Simultaneous thermal analyzer). Samples were heated in corundum crucibles from ambient temperature to 450 °C (10 °C. min^{-1}) in argon (flow 3 ml. min^{-1}).

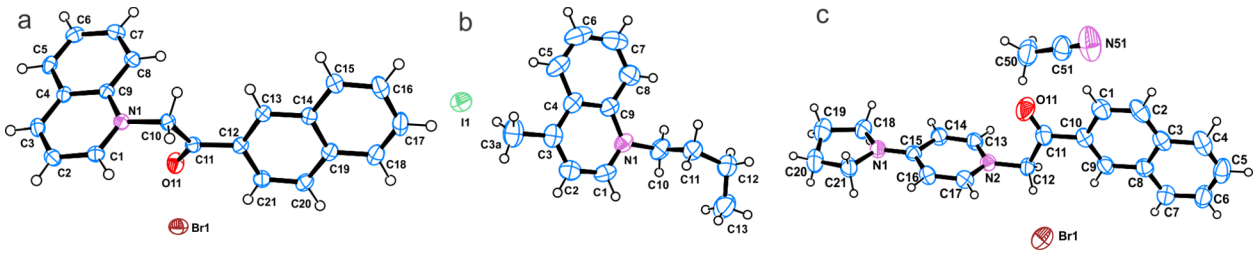

Fig. 1. ORTEP views of the molecules in the asymmetric unit (ASU) of the crystal structures of *a*) compound **1,** *b*) compound **2** and *c*) compound **3**. Atomic displacement parameters (ADP) are drawn at the 50% probability level. Hydrogen atoms are shown as spheres with arbitrary radii.

Table 1. Most important crystallographic parameters for structures **1–3**

Compound	**1**	**2**	**3**
Empirical formula	$C_{21}H_{16}NOBr$	$C_{14}H_{18}IN$	$C_{23}H_{24}N_3OBr$
Formula weight	378.26	327.19	438.36
Temperature/K	150	290	290
Crystal system	Monoclinic	Monoclinic	Monoclinic
Space group	$P2_1/c$	$P2_1/n$	$P2_1/c$
a/Å	15.7293(3)	12.1430(3)	11.2019(4)
b/Å	6.00109(8)	10.0037(2)	8.8763(4)
c/Å	18.4778(4)	12.1552(3)	21.9460(8)
α/°	90	90	90
β/°	104.674(2)	106.648(2)	102.159(4)
γ/°	90	90	90
Volume/Å^3	1687.29(6)	1414.66(5)	2133.17(16)
Z	4	4	4
ρ_{calc} (g/cm^3)	1.489	1.536	1.365
μ/mm^{-1}	3.361	17.571	1.945
F(000)	768.0	648.0	904.0
Crystal size/mm^3	0.25 × 0.2 × 0.2	0.3 × 0.25 × 0.12	0.3 × 0.25 × 0.15
Radiation, λ [Å]	Cu$K\alpha$, 1.54184	Cu$K\alpha$ 1.54184	Mo$K\alpha$, 0.71073
2Θ range for data collection/°	5.808–148.83	9.076 to 149.132	5.908–58.086
Index ranges	$-17 \le h \le 19$, $-7 \le k \le 6$, $-22 \le l \le 17$	$-15 \le h \le 12$, $-12 \le k \le 12$, $-10 \le l \le 15$	$-13 \le h \le 13$, $-11 \le k \le 8$, $-23 \le l \le 29$
Reflections collected/ independent	5828 /3325	9023/2811	9642/4718
R_{int}/ R_{sigma}	0.0208/0.0246	0.0288/ 0.0204	0.0295/0.0456
Data/restraints/parameters	3325/0/281	2811/0/147	4718/0/258
Goodness-of-fit on F^2	1.080	0.901	0.940
Final R indexes [I>=2σ (I)]	R_1 = 0.0328, wR_2 = 0.1148	R_1 = 0.0285, wR_2 = 0.0963	R_1 = 0.0461, wR_2 = 0.1306
Final R indexes [all data]	R_1 = 0.0364, wR_2 = 0.1274	R_1 = 0.0307, wR_2= 0.1053	R_1 = 0.0853, wR_2 = 0.1595
Largest diff. peak/hole / e Å^{-3}	0.53/–0.80	0.73/–0.46	0.28/–0.23
CCDC number	1875087	1875088	1875089

RESULTS AND DISCUSSION

The design of compounds **1**, **2** and **3** has been carried based on the 2-acetonaphthanone and quinoline fragments. Thus a quinoline fragment is present in **1** and **2** while 2-acetonaphthanone moiety is available in **1** and **3**. The concept was to compare the SAR e.g. antimicrobial effect of the two fragments. The compounds were synthesized by facile one-step Menshutkin reaction adapted for aromatic tertiary amines. The inert (argon) atmosphere was necessary because one of the reagents, namely 2-bromo-2'-acetonapthone and butyl iodide, are sensitive to hydrolysis. All starting reagents of the synthesis are highly soluble in the reaction medium (DCE or ACN) therefore the end of the reaction was marked by the formation of colored precipitate (orange – **1**, green – **2** or white – **3**). The purification procedure consisted of consecutive washes with solvent and resulted in good yields (65% – **1**, 78% – **2** and 77% – **3**). The purity of the products was confirmed by ^{1}H-NMR and ^{13}C NMR techniques. The compounds (**1–3)** show no signs of conformational differences due to the changeovers from solution to solid crystalline state which is confirmed by comparing the data from NMR and X-ray studies. Compounds **1** and **2** crystalize in the monoclinic $P2_1/c$ and $P2_1/n$ space groups with one molecule in the asymmetric unit and four molecules in the unit cell (Z=4). The bonds lengths, angles and torsion angles are comparable with those of other similar structures in the Cambridge Structural Database [34–36]. The angle between the mean planes of the quinoline and naphthalene moieties in **1** is 67.44° while the angle between quinoline and butyl fragments in **2** is 54.98°. Overlay of the molecules of **1**

Table 2. Selected bond lengths, angles and torsion angles for structures **1–3**

Structure	1	2	Structure	3
Bond lengths (Å)	Å	Å	*Bond lengths* (Å)	Å
N1—C10	1.476 (2)	1.488 (3)	N1—C12	1.462 (3)
N1—C9	1.388 (2)	1.385 (4)	N2—C15	1.333 (3)
N1—C1	1332 (3)	1.328 (4)	N1—C17	1.348 (3)
C12—C11	1.492 (3)	1.524 (4)	C19—C20	1.453 (6)
C10—C11	1.516 (3)	1.520 (4)	N2—C18	1.467 (4)
O11—C11	1.215 (2)	–	O11—C11	1.204 (4)
Angles	°	°	*Angles*	°
C13—C12—C11	122.05 (18)	113.8 (3)	C13—N1—C12	120.5 (2)
O11—C11—C12	121.75 (18)	–	C17—N1—C12	120.2 (2)
O11—C11—C10	121.06 (18)	–	C15—N2—C18	123.9 (2)
N1—C10—C11	110.47 (16)	112.4 (2)	C15—N2—C21	123.9 (2)
C9—N1—C10	120.02 (16)	122.3 (2)	O11—C11—C10	121.3 (3)
C1—N1—C9	121.65 (17)	120.7 (2)	O11—C11—C12	121.4 (3)
Torsion angles	°	°	*Torsion angles*	°
C9—N1—C10—C11	−81.7 (2)	90.2 (3)	C18—C19—C20—C21	25.7 (5)
N1—C10—C11—O11	−8.4 (3)	–	C18—N2—C15—C14	3.7 (4)
C13—C12—C11—C10	−26.6 (3)	−69.5 (4)	C13—N1—C12—C11	84.1 (3)

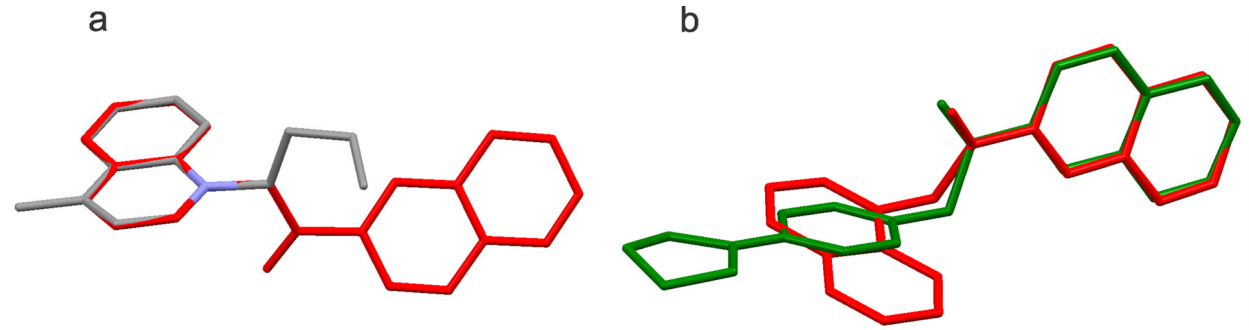

Fig. 2. Overlay of the molecules of a) compounds **1** – red and **2** – gray by their identical quinoline fragment and b) compounds **1** – red and **3** – green by the 2-acetonaphthanone fragment.

and **2** by their identical quinoline fragment (Fig. 2a) shows that butyl and 2-acetonaphthanone fragments are oriented on the opposite sides of the mean plane of the quinoline moiety.

The lack of classical donors and acceptors determines the absence of typical hydrogen bonding interactions. Instead, the crystal structures of **1** and **2** are stabilized by a network of intermolecular halogen interactions (C-H...X, X= Br for **1** and X= I for **2**, Table 3, Fig. 3).

As a result of these interactions, three-dimensional packaging of molecules of **2** generates channels (pores) oriented along the *a*-axis (Fig. 4b) where the I-anions are situated. The molecule of **1** is build up by two aromatic rings connected by CH_2–CO–C bridge, however no bulky substituents are present. Thus the three-dimensional packaging of molecules (Fig. 4a) is governed only by the halogen bonding interactions and does not require the formation of pores or channels to accommodate the bulkier alkyl moieties (CH_3 or butyl) present in **2**.

The stabilizing (indispensable, structural) role of the bromine and iodine anions is confirmed by the DTA/TG analysis (Fig. 5). The DTA curve for **1** (Fig. 5a) shows two *endo* effects at 235 °C and 259 °C. They correspond first to the melting of the crystal followed by the removal of bromine anion. TGA registered a sharp decrease of the weight of **1** (up to ~70% *wt*) that starts immediately after the melting point. Similarly, DTA curve of **2** (Fig. 5b) shows a sharp *endo* effect at 120 °C due to the melting of the crystal and broad *endo* effect at 252 °C corresponding to the loss of iodine anions (~40% weight loss) followed by fast destruction of the crystal. The decomposition, starting immediately after bromine and iodine removal, is an important

Table 3. Halogen bonding interactions for **1** and **2**

		1		
D—H···A	D—H	H···A	D···A	D—H···A
C1—H1···Br1	0.92 (3)	2.82 (3)	3.695 (2)	159 (2)
C10—H10A···Br1	0.92 (2)	2.80 (3)	3.587 (2)	144.7 (19)
C2—H2···Br1^{i}	0.90 (3)	2.89 (3)	3.779 (2)	170 (2)
C10—H10B···Br1^{ii}	0.97 (3)	2.74 (3)	3.6327 (19)	153.2 (19)
Symmetry operations: *(i) −x, −y, −z; (ii) x, y+1, z.*				
		2		
C1—H1···I1^{i}	0.93	3.16	3.830 (3)	130
C1—H1···I1^{ii}	0.93	3.13	3.648 (3)	117
C8—H8···I1^{iii}	0.93	3.03	3.906 (4)	157
C10—H10B···I1^{i}	0.97	3.14	4.050 (3)	156
Symmetry operations: *(i) −x+1/2, y−1/2, −z+3/2; (ii) x+1/2, −y+3/2, z+1/2; (iii) x, y−1, z.*				

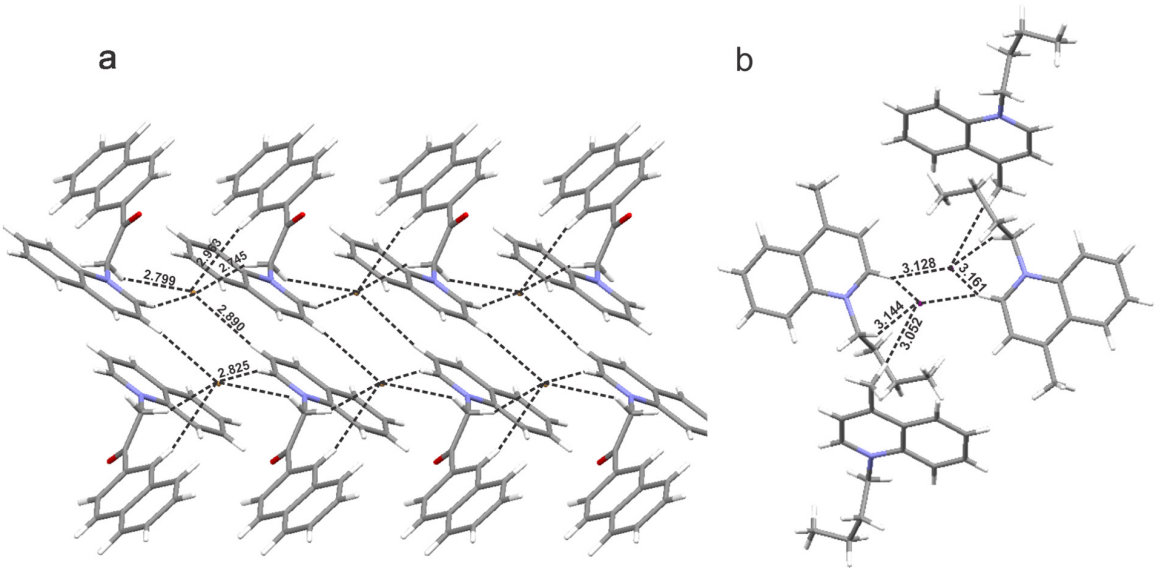

Fig. 3. Network of halogen bonding interactions stabilizing the structures of a) compound **1** and b) compound **2**. The H…X distances are given in Å.

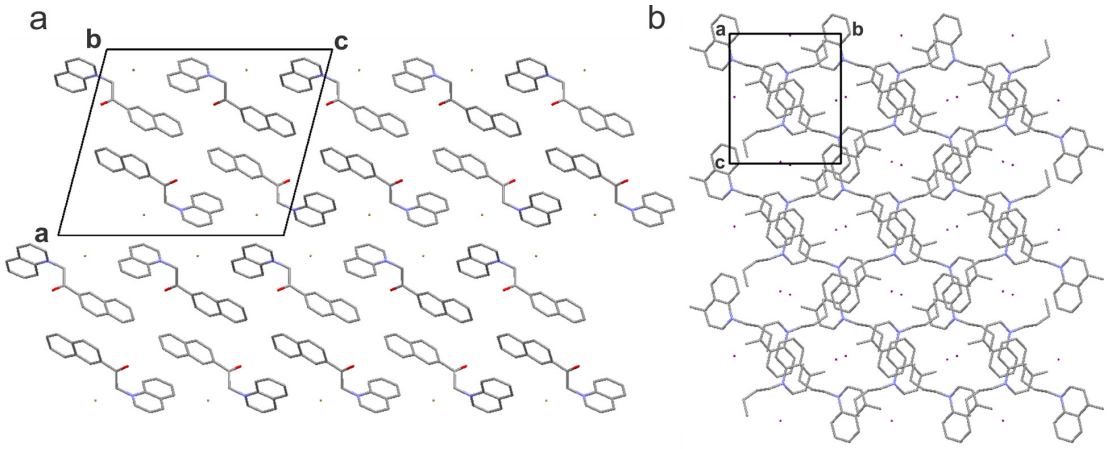

Fig. 4. Three dimensional packing of the molecules in the crystal structure of a) – **1** along axis *b* and b) – **2** along axis *a* (hydrogen atoms were omitted from the figures)**.** One can notice the presence of cavities in **2** in which the counter iodine ions are located.

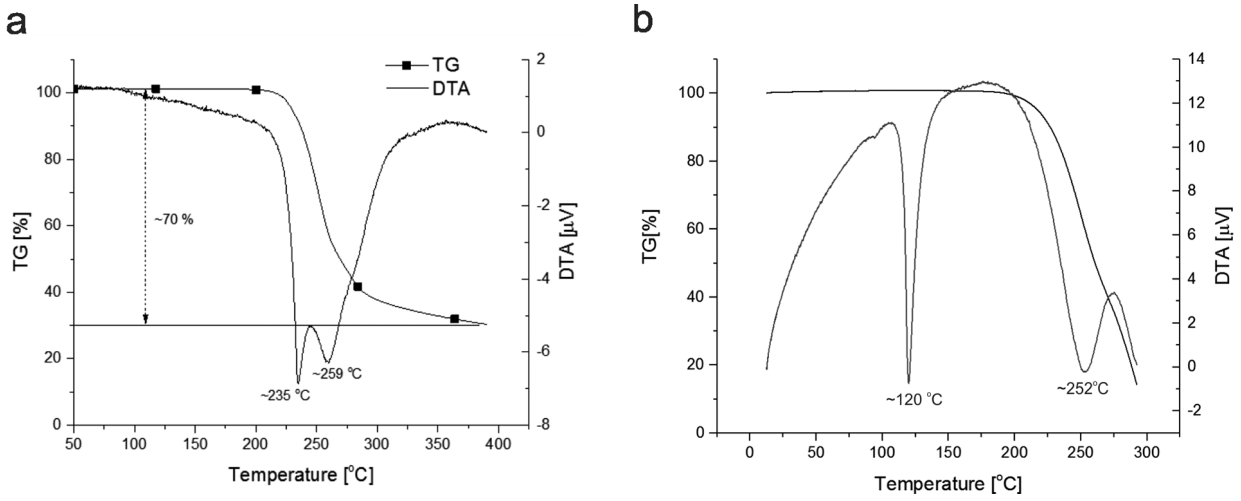

Fig. 5. DTA/TG curves for a) – compound **1** and b) – compound **2**.

proof of their role in the stabilization of the crystal structures of **1** and **2**.

Compound **3** crystalizes in monoclinic $P2_1/c$ space group with one molecule in the ASU and four molecules in the unit cell (Z=4). The molecule of the solvent (Acetonitrile) employed during the reaction is also present in the unit cell. Actually the structural difference between compound **1** and **3** is the longer – 4-(pyrrolidin-1-yl) pyridine ring system. Indeed, the angle between the mean planes of the 4-pyrolidino pyridine and naphthalene moieties is almost perpendicular – 88.86° while the angle between the mean planes of the quinoline and naphthalene moieties in **1** is 67.44°. This is reflected by a minor shift in the orientation of the corresponding quinoline and 4-pyridino pyridine moieties visible on the overlay of **1** and **3** (shown on Fig. 2b) based on their identical 2-acetonaphthanone fragments. Similarly, to **1** in **3** there are no bulky or flexible alkyl fragments and thus no pores or channels are generated by the three dimensional arrangement of the molecules in the crystal structure. For **3** the crystal packing of the molecules is also governed by the halogen bonding interactions (Table 4). The interactions produce a *zig-zag* orientation of the molecules along the *c-axis* (Fig. 6).

Three distinct *endo*-thermal effects at ~81 °C, ~281 °C and ~310 °C can be observed from the DTA/TG curve of compound **3** (Fig. 7). The thermal effect at 81 °C is due to acetonitrile leaving the crystal structure. The sharp effect observed at 281 °C is associated with the melting of the crystal. Finally, the broad effect registered around 310 °C corresponds to release of the bromine anion followed by an immediate destruction of the compound. The TGA registered total weight losses are about 71% of the starting mass of which 8% are due to the acetonitrile leaving. An interesting fact is that acetonitrile departs the crystal structure at the same temperature as the boiling of pure ACN which is an evidence for very weak interactions between the molecule of the solvent and the quaternary ammonium compound.

Table 4. Halogen bonding interactions for **3**

D—H···A	D—H	H···A	D···A	D—H···A
C16—H16···N51^{i}	0.93	2.49	3.282 (4)	144
C13—H13···Br1^{ii}	0.93	3.11	3.925 (3)	148
C12—H12A···Br1^{ii}	0.97	2.79	3.659 (3)	149
C12—H12B···Br1	0.97	2.77	3.658 (3)	153
C17—H17···Br1	0.93	3.08	3.917 (3)	151
C50—H50A···Br1^{i}	0.96	2.95	3.877 (4)	162
C50—H50C···Br1^{iii}	0.96	3.12	3.919 (4)	142
Symmetry operations: *(i) −x+1, −y, −z; (ii) −x+1, y−1/2, −z+1/2; (iii) x, y−1, z.*				

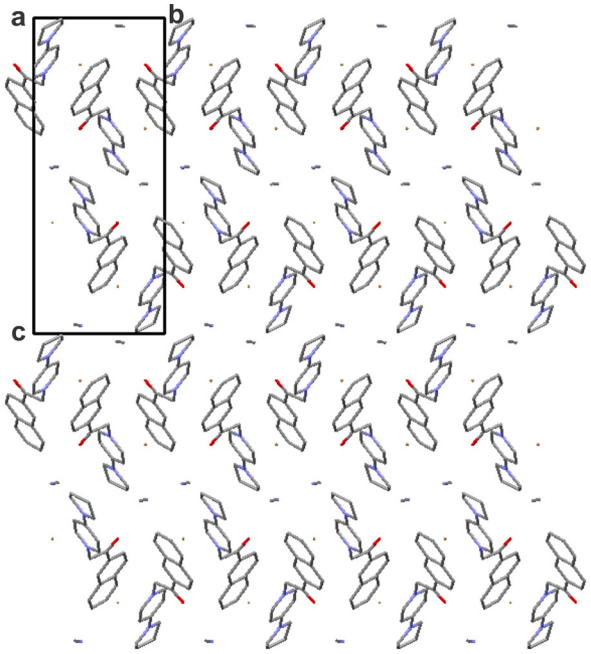

Fig. 6. Three dimensional packing of the molecules in the crystal structure of **3** (hydrogen atoms were omitted from the figures). One can observe *zig-zag* orientation of the molecules along the *c*-axis.

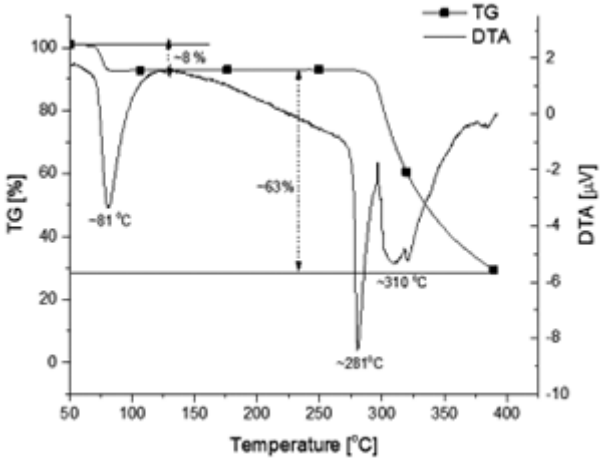

Fig. 7. DTA/TGA curves for structure **3**.

Antibacterial study

Bacterial strains synthesizing metabolic components such as organic acids, hydrogen peroxide and bacteriocins exhibit resistance to currently used antibacterial agents. Therefore, antibacterial activity is a desirable property and a plethora of compounds have been designed and synthesized in order to achieve higher bacterial susceptibility. Compounds **1-3** were tested for antibacterial activity against Gram positive bacteria – *Bacillus subtilis* and *Staphylococcus aureus* and Gram negative bacteria – *Escherichia coli* and *Klebsiella pneumoniae* using Kirby- Bauer disk diffusion test according to Clinical and Laboratory Standards Institute [37]. Mueller – Hinton agar was autoclaved (121°C, 1.5 *atm* for 30 minutes) and used as a microbiological growth medium.

Disk – diffusion method

Bacterial suspension in liquid growth medium with concentration of ~1.10^7 *cfu*/ml was prepared. A volume of 12–16 ml of warm (50–55 °C) Muller Hinton agar (~1.5% agar) medium was poured into 90 mm sterile Petri dishes. After solidification and cooling of the medium, 0.2 ml of the bacterial suspension was gently spread on the surface using cell spreader. Sterile cellulose discs (6 mm in diameter) were submerged in test compound solutions (10 µM) and were placed on the growth medium. The plates are then incubated at 37 °C for 24 h. The diameters of the areas around the wells in which no growth is observed were measured. The size of the inhibition zones (Table 5) was measured with ImageJ software [38]. Compounds exhibiting zones without observed bacterial growth with a diameter greater than 5–6 mm are assumed to possess inhibition properties.

Minimal (MIC) and non-inhibitory (NIC) concentrations

MIC is the lowest concentration which prevents the visible growth of the bacterium. Broth micro dilution test was performed in plastic 96 well flat bottom plates (Sarstedt, 83.1835.50) using 10 µM of the test compounds **1–3**. The plates were incubated for 24 hours at 37 °C, afterward the optical density at 600 nm (Bio-Tek ELx800, Universal Microplate Reader) was determined. The Gompertz function [39] is used to model the inhibition profiles from data using two principle parameters: the inflexion point of the function and the slope. The graphical representation of the Gompertz fit for calculation of MIC and NIC of **2** (most active compound) is shown on Fig. 8. The values for MIC and NIC for compounds **1–3** are summarized in Table 6.

CONCLUSIONS

Three novel aromatic quaternary ammonium compounds have been synthesized by facile one step synthesis as bromine or iodine salts. The single crystal X-ray diffraction study determined that

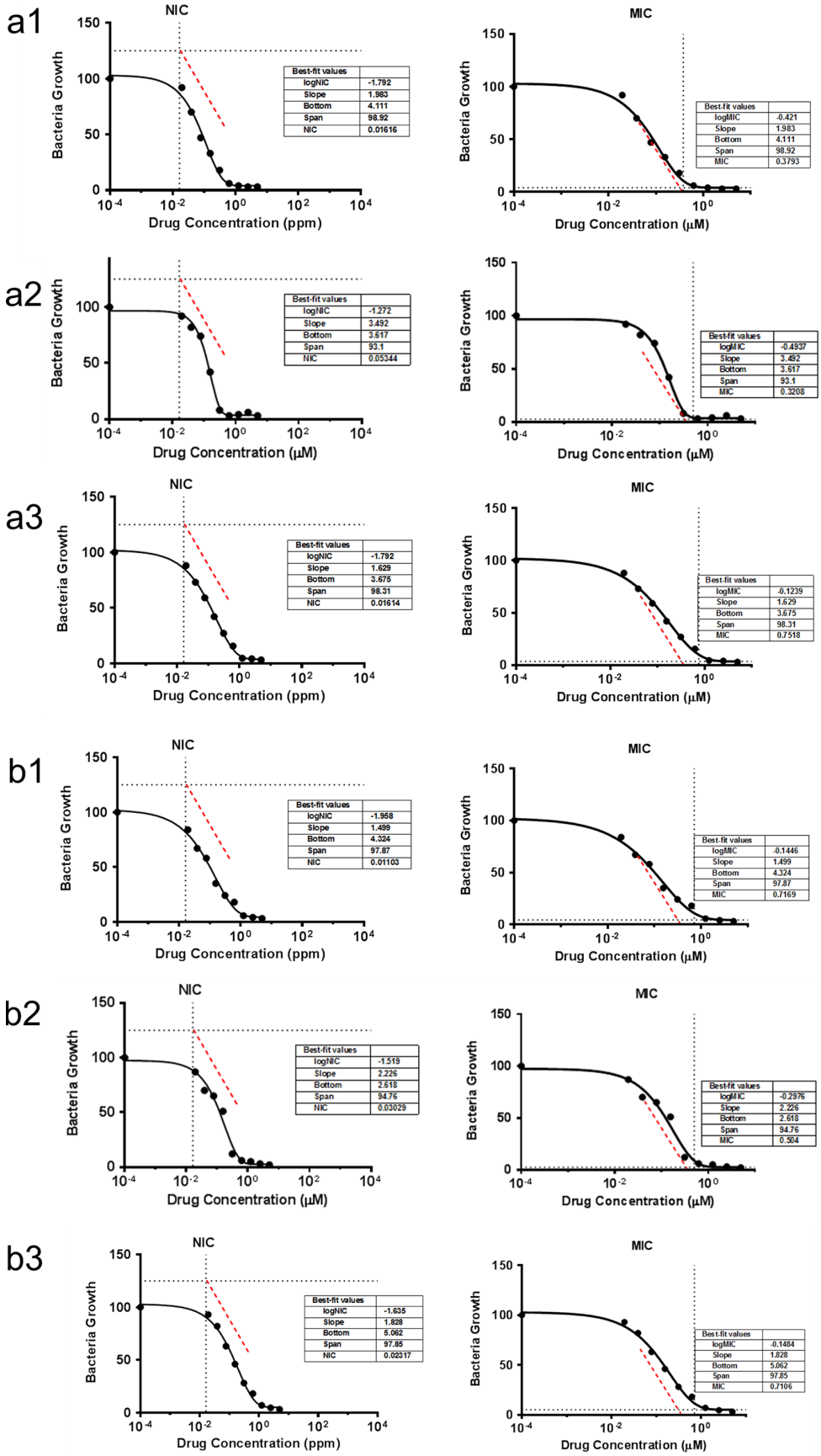

Fig. 8. Graphical representation of the Gompertz fit for calculation of minimum inhibitory concentration (MIC) and non-inhibitory concentration (NIC) of **1, 2** and **3** against *a*) – *Staphylococcus aureus* and *b*) – *Bacillus subtilis*.

Table 5. Inhibition zone (mm) for compounds **1**, **2** and **3** against Gram-positive bacteria – *Bacillus subtilis* and *Staphylococcus aureus* and Gram-negative – *Escherichia coli* and *Klebsiella pneumoniae* using disc-diffusion method

	Inhibition zone (mm)			
Compound \ Bacteria	*Staphylococcus aureus*	*Bacillus subtilis*	*Escherichia coli*	*Klebsiella pneumoniae*
1	15	10	2	–
2	18	15	5	2
3	16	8	–	–

Table 6. MIC and NIC for compounds **1–3**

	MIC [μM]	
Compound \ Bacteria	*Staphylococcus aureus*	*Bacillus subtilis*
1	0.379	0.755
2	0.321	0.504
3	0.717	0.710
	NIC [μM]	
1	0.16	0.16
2	0.05	0.03
3	0.01	0.02

their crystal structures are stabilized by a network of strong intermolecular halogen bonding. The compounds were tested for antibacterial activity against Gram-negative and Gram-positive bacterial strains. QAS showed moderate growth inhibition properties against the Gram-positive bacteria – *Staphylococcus aureus* and *Bacillus subtilis* and lower antibacterial effect against the Gram-negative – *Escherichia coli* and *Klebsiella pneumoniae*.

REFERENCES

1. J. L. M. Abboud, R. Notario, J. Bertrán, M. Solà, *Progr. Phys. Org. Chem.*, **19**, 7 (1990).
2. E. M. Arnett, R. Reich, *J. Am. Chem. Soc.*, **102**, 5892 (1980).
3. M. Sola, A. Lledos, M. Duran, J. Bertran, J. L. M. Abboud, *J. Am. Chem. Soc.*, **113**, 2873 (1991).
4. L. Deady, *Aust. J. Chem.*, **26**, 1949 (1973).
5. B. Trivedi, A. Digioia, P. Menardi, *J. Am. Oil Chem. Soc.*, **58**, 754 (1981).
6. J. Rippey, M. Stallwood, *Emerg. Med. J.*, **22**, 878 (2005).
7. Y. Jiang, T. Geng, Q. Li, *J. Surfactants Deterg.*, **15**, 67 (2012).
8. Z. Zheng, T. Wu, X. Zhou, *Chem. Commun.*, 1864 (2006).
9. F. M. Menger, J. S. Keiper, *Angew. Chem. Int. Ed.*, **39**, 1906 (2000).
10. B. Lygo, B. I. Andrews, *Acc. Chem. Res.*, **37**, 518 (2004).
11. S. Mishra, *J. Oleo Sci.*, **56**, 269 (2007).
12. Z. B. Zhou, H. Matsumoto, K. Tatsumi, *Chem. Eur. J.*, **12**, 2196 (2006).
13. H. Sakaebe, H. Matsumoto, *Electrochem. Commun.*, **5**, 594 (2003).
14. R. J. Fair, Y. Tor, *Perspect. Med. Chem.*, **6**, PMC. S14459 (2014).
15. S. A. Chisholm, J. Dave, C. A. Ison, *Antimicrob. Agents Chemother.*, **54**, 3812 (2010).
16. K. S. Long, B. Vester, *Antimicrob. Agents Chemother.*, **56**, 603 (2012).
17. C. M. Thomas, K. M. Nielsen, *Nat. Rev. Microbiol*, **3**, 711 (2005).
18. J. R. Huddleston, *Infect. Drug Resist.*, **7**, 167 (2014).
19. B. Deslouches, J. D. Steckbeck, J. K. Craigo, Y. Doi, J. L. Burns, R. C. Montelaro, *Antimicrob. Agents Chemother.*, **59**, 1329 (2015).
20. A. C. Rios, C. G. Moutinho, F. C. Pinto, F. S. Del Fiol, A. Jozala, M. V. Chaud, M. M. Vila, J. A. Teixeira, V. M. Balcão, *Microbiol. Res.*, **191**, 51 (2016).
21. M. F. Chellat, L. Raguž, R. Riedl, *Angew. Chem. Int. Ed.*, **55**, 6600 (2016).
22. T. Thorsteinsson, M. Másson, K. G. Kristinsson, M. A. Hjálmarsdóttir, H. Hilmarsson, T. Loftsson, *J. Med. Chem.*, **46**, 4173 (2003).
23. J.-Y. Sun, J. Li, X.-L. Qiu, F.-L. Qing, *J. Fluorine Chem.*, **126**, 1425 (2005).
24. L. Massi, F. Guittard, S. Géribaldi, R. Levy, Y. Duccini, *Int. J. Antimicrob. Agents*, **21**, 20 (2003).
25. B. Dizman, M. O. Elasri, L. J. Mathias, *J. Appl. Polym. Sci.*, **94**, 635 (2004).
26. S. P. Denyer, *Int. Biodeterior. Biodegrad.*, **36**, 227 (1995).
27. S. Buffet-Bataillon, P. Tattevin, M. Bonnaure-Mallet, A. Jolivet-Gougeon, *Int. J. Antimicrob. Agents*, **39**, 381 (2012).
28. K. Hegstad, S. Langsrud, B. T. Lunestad, A. A. Scheie, M. Sunde, S. P. Yazdankhah, *Microb. Drug Resist.*, **16**, 91 (2010).
29. K. Poole, *Ann. Med.*, **39**, 162 (2007).
30. L. J. Piddock, *Nat. Rev. Microbiol*, **4**, 629 (2006).
31. G. M. Sheldrick, *Acta Crystallogr. Sect. A: Found. Crystallogr.*, **64**, 112 (2008).

32. L. J. Farrugia, *J. Appl. Crystallogr.*, **45**, 849 (2012).
33. C. F. Macrae, P. R. Edgington, P. McCabe, E. Pidcock, G. P. Shields, R. Taylor, M. Towler, J. v. d. Streek, *J. Appl. Crystallogr.*, **39**, 453 (2006).
34. A. Schmidt, T. Mordhorst, M. Nieger, *Org. Biomol. Chem.*, **3**, 3788 (2005).
35. C. Ni, D. Dang, Z. Ni, Z. Tian, Y. Li, J. Xie, Q. Meng, Y. Yao, *J. Coord. Chem.*, **57**, 705 (2004).
36. Y. Chen, Q.-y. Chen, M.-h. Chen, X.-s. Chen, J.-r. Zhou, C.-l. Ni, *Chem. Res.*, **5**, 010 (2012).
37. M. A. Wikler, *Performance standards for antimicrobial disk susceptibility tests: Approved standard* (Clinical and laboratory standards institute, 2006).
38. C. A. Schneider, W. S. Rasband, K. W. Eliceiri, *Nat. Methods*, **9**, 671 (2012).
39. R. Lambert, J. Pearson, *J. Appl. Microbiol.*, **88**, 784 (2000).